Astron. Astrophys. 354, 1062–1070 (2000)

ASTRONOMY AND ASTROPHYSICS

Hydrocarbons in diffuse and translucent clouds

S. Viti, D.A. Williams, and P.T. O'Neill

Department of Physics and Astronomy, UCL, Gower St., London, WC1E 6BT, UK

Received 18 October 1999 / Accepted 29 November 1999

Abstract. We investigate the consequences on hydrocarbon chemistry in diffuse and translucent clouds of including an interaction between gaseous C^+ ions and dust grains. In general, we find that models in which much of the carbon is deposited and retained on grain surfaces within the cloud lifetime represent a poor match to observations. Conversely, models in which carbon is efficiently converted to methane generally provide satisfactory agreement with the observed chemistry of translucent clouds. Such models also predict that the hydrocarbons C_2H, C_3H_2 and H_2CO may be detectable in diffuse clouds.

Key words: molecular processes – ISM: abundances – ISM: molecules

1. Introduction

Diffuse interstellar clouds are detected towards bright background sources in the absorption lines of various species such as CO, OH, CH, CH^+, CN and CS (e.g. van Dishoeck & Black 1989; Lambert & Danks 1986; Drdla, Knapp & van Dishoeck 1989). Model calculations of diffuse interstellar clouds have been quite successful in reproducing the observed abundances of such species (e.g. Wagenblast & Williams 1996 and references therein), with the exception of CH^+. Hydrocarbons, in particular CH and CH^+, have been the subject of several studies. CH is especially important as it was found to have a linear relation with H_2 (Danks, Federman & Lambert 1984) but CH^+ remains an anomaly (Williams 1992). So far, chemical models have reproduced the observed abundances of hydrocarbons in diffuse clouds *via* simple chemical networks involving photodissociation, photoionization, and reactions with atomic and molecular hydrogen and electrons. To date, the only observable hydrocarbons with reported column densities measurements, are CH and CH^+, but a variety of others might be present, such as CH_2, CH_3, CH_4, small molecules containing two or three carbon atoms, and PAHs.

Translucent clouds ($A_v \sim 2$–5 mag) have been less well studied but appear to extend the diffuse cloud population to larger visual extinctions (Snow et al. 1996). They are characterized by larger molecular column densities than those inferred for diffuse clouds. To date, many hydrocarbons have been detected, in particular CH (Magnani & Onello 1993); C_3H_2 (Turner, Lee, & Herbst 1998); CH_3OH (Turner 1998); and C_2H (Turner et al. 1999).

Carbon plays an important role in determining the column densities of hydrocarbons in the gas phase and/or on grains. Its fractional abundance (relative to H nuclei) has been accurately determined by surveys of F and G stars (Snow & Witt 1996) and it is found to be 2×10^{-4}, somewhat less than the solar value. This revised (lower) abundance of carbon is a severe constraint on chemical models.

Hydrocarbons form in the gas phase *via* the following network (cf. van Dishoeck 1998):

$$\begin{array}{ccccccc} C^+ & \xrightarrow{H_2} & CH_2^+ & \xrightarrow{H_2} & CH_3^+ & \xrightarrow{H_2} & CH_5^+ \\ & & \downarrow e & & \downarrow e & & \downarrow e \\ & & CH & & CH, CH_2 & & CH_3 \end{array}$$

These routes involve two slow radiative associations of ions with H_2. For these to be efficient enough for the network to reproduce the observed abundance of CH, nearly all of the carbon must be in the gas phase and ionized. Recent detailed models of the diffuse clouds towards ζ Oph and ξ Per (Wagenblast & Williams 1996) additionally required that the recombination coefficient of C^+ be lowered by at least a third from the canonical high temperature value. It is also implicit in these models that carbon is retained in the gas and does not freeze–out on to grains. These models have been able to reproduce successfully many of the observed species in these lines of sight (Wagenblast & Williams 1993, 1996).

However, alternative routes might be available for hydrocarbons to form, such as surface reactions. Freeze–out of gas species and surface reactions in the diffuse clouds have not been fully explored but may be significant. In fact, there is some evidence that surface reactions are important in producing the observed amount of NH; its observed abundance on several diffuse lines of sight can only be explained by assuming that some of the nitrogen that depletes onto grains is hydrogenated and released into the gas (Wagenblast et al. 1993; Crawford & Williams 1997). Models including oxygen hydrogenation on grain surfaces, forming OH or H_2O, have also been explored and shown to be viable (Wagenblast & Williams 1993, 1996).

Send offprint requests to: sv@star.ucl.ac.uk

A question that has not so far been addressed in this context is the interaction of carbon with dust. In diffuse clouds nearly all the available carbon at low visual extinction is photoionized, and chemical models of diffuse clouds have therefore generally assumed that carbon is not depleted on the dust. On the other hand, a class of grain models has assumed that carbon is depleted in the form of hydrogenated amorphous carbon (HAC) mantles on silicate cores (Jones et al. 1990). In these models, it is assumed that significant loss of carbon from the gas into HAC mantles occurs in diffuse clouds on a timescale of around 10My. Thus, extinction in these models becomes a time–dependent property (Cecchi–Pestellini & Williams 1998). Diffuse cloud chemistry would also be, in this case, time–dependent on a similar timescale. On the other hand, it may be that carbon is fully hydrogenated on the surfaces of dust grains, and returned to the gas phase, as is implied by the NH observations. It is unclear, at present, which of these processes (if either of them) is occurring.

The purpose of this paper is, therefore, to investigate the viability of diffuse and translucent cloud models in which carbon is either continually incorporated into HAC mantles or is returned to the gas phase as CH_4. Note that in translucent clouds not all the carbon is ionized. The production of CH_4 on grains and its release should therefore be less with respect to the diffuse cloud case.

We predict the abundances of polyatomic hydrocarbons and some simple chemical derivatives of these species. Sect. 2 contains a description of the chemical model, and Sect. 3 presents the results and some discussion. Sect. 4 gives a brief conclusion.

2. The model

We model the chemistry of a diffuse cloud represented as a semi–infinite slab, with a pseudo–time–dependent multi–point chemical simulation. The UMIST chemical database (Millar et al. 1997) was used, with the following modifications:

(i) We have removed the reactions:

$$CH_5^+ + e \rightarrow CH_4 + H \quad (1)$$

$$CH_5^+ + e \rightarrow CH_3 + H_2 \quad (2)$$

and replaced them with the following:

$$CH_5^+ + e \rightarrow CH_3 + H + H \quad (3)$$

$$CH_5^+ + e \rightarrow CH_2 + H_2 + H \quad (4)$$

Recently, Semaniak et al. (1998) measured the absolute dissociative recombination and excitation cross sections for CH_5^+ and found that reactions 1 and 2 do not occur and that reactions 3 and 4 dominate over other dissociation channels with the same rate coefficients as those of reactions 1 and 2. The obvious gas phase route to CH_4 is, therefore, suppressed.

(ii) We have included the freeze–out of all gas phase species, except hydrogen and helium, onto dust grains. All the species that deplete onto grains are incorporated in mantles and never released except for C^+ which either hydrogenates on the grains to CH_4 and is immediately released into the gas, entering the gas phase chemical network, or is retained in HAC.

The modified rate file contains 394 gas species taking part in 4247 reactions (including freeze–out reactions). CO self–shielding was accounted for by the method of Wagenblast (1992). Typical densities for diffuse clouds are 100-300 cm^{-3} (Wagenblast & Williams 1993); for translucent clouds they might be higher; we have used a uniform number density, n_H = n(H) + 2n(H_2) of 300 cm^{-3}. In all models the initial elemental abundances by number relative to hydrogen were taken to be 7.0×10^{-2}, 1.1×10^{-4}, 6.0×10^{-5}, 4.6×10^{-4}, 1.3×10^{-5}, 3.0×10^{-9}, 2.0×10^{-7} and 7.0×10^{-9} for helium, carbon, nitrogen, oxygen, sulphur, magnesium, sodium, and silicon respectively. For each model we have performed several runs to cover visual extinctions from 0 to 4 mags in order to estimate column densities in both diffuse and translucent clouds. In fact, for diffuse clouds the visual extinction does not normally exceed $\sim$ 1 mag (cf. van Dishoeck 1998) while translucent clouds typically have somewhat larger visual extinctions (2–5 mag, Snow et al. 1996). Our models are time and depth dependent; this implies that the depletion of each element is not assumed but it is derived by a non–steady state computation of the chemical evolution of the gas/dust interaction processes. Also the abundances that we derive for translucent clouds are directly computed from the initial cosmic abundances. Our initial H/H_2 ratio varies with visual extinction according to the total molecular hydrogen number density profile found by Wagenblast & Hartquist (1988). For $A_v \geq 0.5$mags and for densities of 300 cm^{-3} (when the cloud is already in its diffuse state) nearly all the hydrogen is found to be in molecular form.

We have computed the chemical behaviour for three models:
Model A: C^+ + grain $\rightarrow$ HAC
Model B: C^+ + grain $\rightarrow$ $CH_4 \uparrow$
Model AB: C^+ + grain $\rightarrow$ HAC (50%) + $CH_4 \uparrow$ (50%)
In these models, hydrocarbons and their derivatives are the products of a combination of (i) dissociation of the CH_4 formed on grains and (ii) gas phase reactions involving ionized carbon. We assume that on its arrival on grains, C^+ will react with hydrogen forming CH which, due to its valence, will stay bound to the surface where it will have enough time to continue reactions with hydrogen, eventually forming CH_4. The latter molecule is unlikely to remain bound to the grains; its binding energy to the surface is relatively small, but the energy released in the final stage of hydrogenation is relatively large. We have investigated the effects and consequences of our models and we propose ways of determining the extent, if any, to which Model B may be important for abundances of hydrocarbons and their derivatives in diffuse and translucent clouds. Evidently, for models A and AB, it is necessary to show the time dependence of the results; no chemical steady state can be obtained. This is the opposite of the usual assumption made for diffuse clouds. Our results are therefore shown in three-dimensional plots.

In most of the calculations, we assume a reduced grain surface area per unit volume and a sticking probability, S_x, of 1 for all species; the depletion rate for ions is enhanced on negatively charged grains according to the expression used by Rawlings

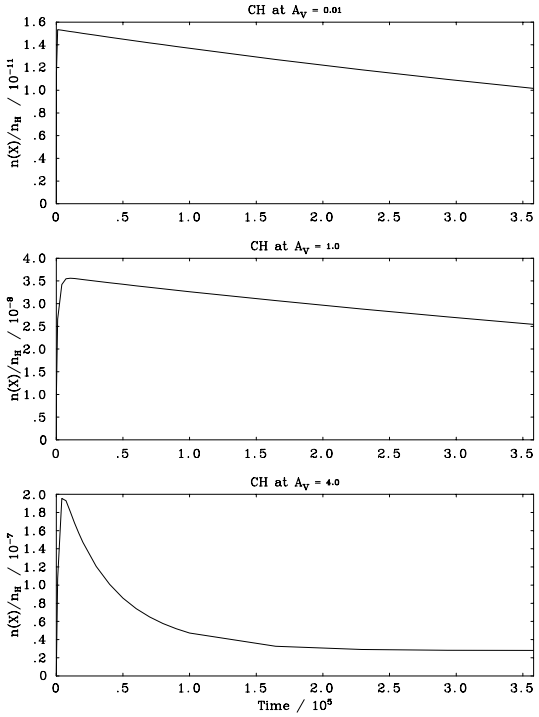

Fig. 1. Fractional abundances of CH for Model A as a function of time at early stages.

et al. (1992). With these choices then, about a third of heavy elements are depleted on to grains in a period of 10 My. Results are dependent on the product of S_x and the amount of cross section provided per unit volume by the adopted grain size distribution. We have also explored the consequences of varying this product.

3. Results

Our results are shown in Figs. 1 – 6, where we plot the fractional abundances of some hydrocarbons and their chemical derivatives as a function of time and visual extinction, and in Table 1 where we list the observed and theoretical estimates of the column densities for all the species analysed in the following sections, up to A_v = 1 (to represent diffuse clouds), and up to A_v = 3 and 4 (to represent translucent clouds). The next two sections will discuss hydrocarbons in diffuse and translucent clouds separately. The figures and the table, however, show them together, with the translucent clouds being represented by the fractional abundances or column densities at higher visual extinctions.

3.1. Diffuse clouds

We first consider CH and make comparisons with observations. Fig. 2 shows three-dimensional plots of fractional abundances of CH as a function of visual extinction and time for the three models. We plot A_v up to a depth where the C^+ abundance is almost insignificant ($A_v \sim$ 4 mags), noting that for diffuse clouds A_v does not normally exceed 1 mag. In Fig. 1 we show the early–time CH fractional abundance as a function of time up to 3×10^5 years, for three different visual extinctions for Model A: A_v = 0.01 (edge of a cloud); A_v = 1 (diffuse state) and A_v = 4 (translucent cloud) while in the other plots, we have chosen to present the evolution of CH abundances after 3×10^5 years, as it is unlikely that we can observe the diffuse clouds at the early stages (t $\leq 3\times10^5$ years). In all three plots of Fig. 1 there is a peak in the abundance at a very early stage ($\sim 10^4$ years); after that, CH starts declining. In fact, in Model A, for visual extinctions typical of diffuse clouds, CH is only reasonably abundant for t $\leq 10^6$ years when all the C^+ is still in the gas. At early times we reproduce the same gas phase environment as Wagenblast & Williams (1996) but without lowering the C^+ recombination rate coefficient.

At visual extinctions of less than 2 mags, CH in model B is at least a factor of 2 more abundant than in model A (see Fig. 2, right plot). Model AB is somewhere in between the two values. If all the depleted C^+ is retained in the HAC mantles, not enough CH is produced in the gas phase.

Fig. 2, bottom and right plots, shows that a detectable amount of CH, comparable to observed quantities, is always reached, even at visual extinctions typical of diffuse clouds. Here, CH is produced via photodissociation of CH_4. In fact, the same behaviour is reproduced in the fractional abundances of CH_4 (direct product of depletion of C^+, see Fig. 3), CH_3 and CH_2 (formed, together with CH via photodissociation of CH_4, not illustrated).

The differences between the three models are more obvious by looking at the column densities of some selected species (Table 1). We have estimated column densities of some of the hydrocarbons for the three models after 10 Myr. We present column densities up to 1 mag (typical for diffuse clouds), 3 mag (typical for translucent clouds) and 4 mag. Table 1 shows our estimates and compares them with observed abundances where possible. The column density of CH for Model B (at A_v = 1 mag) is lower than the observed value by a factor of 5, while the column density of CH for Model A is significantly underabundant. In the models where depletion of C^+ occurs other hydrocarbons such as methane are abundant. Observations of methane would be the most stringent test for determining if depletion and hydrogenation of C^+ occur. However, due to its high degree of symmetry this molecule does not have a permanent dipole moment and so it does not have an observable radio spectrum.

As direct observations of the hydrogenation of C^+ are not possible we may be able to test the hypothesis that CH_4 is made on and released from grain surfaces by detecting its products made in the gas phase. A direct product of photodissociation of methane is CH_3. In the gas phase, CH_3 efficiently reacts with oxygen (still abundant at very late times) to form H_2CO. If C^+ is hydrogenated at grain surfaces then we should see an increase in H_2CO with respect to the scenario pictured in Model A.

H_2CO, as many other species, is an important molecule for the study of dense clouds ($n > 10^3$ cm^{-3}) and recent observations of diffuse clouds (Liszt & Lucas 1999) show that many species, such as HCO^+, HCN, HNC, C_2H and indeed H_2CO, are overabundant, relative to standard diffuse cloud models, by

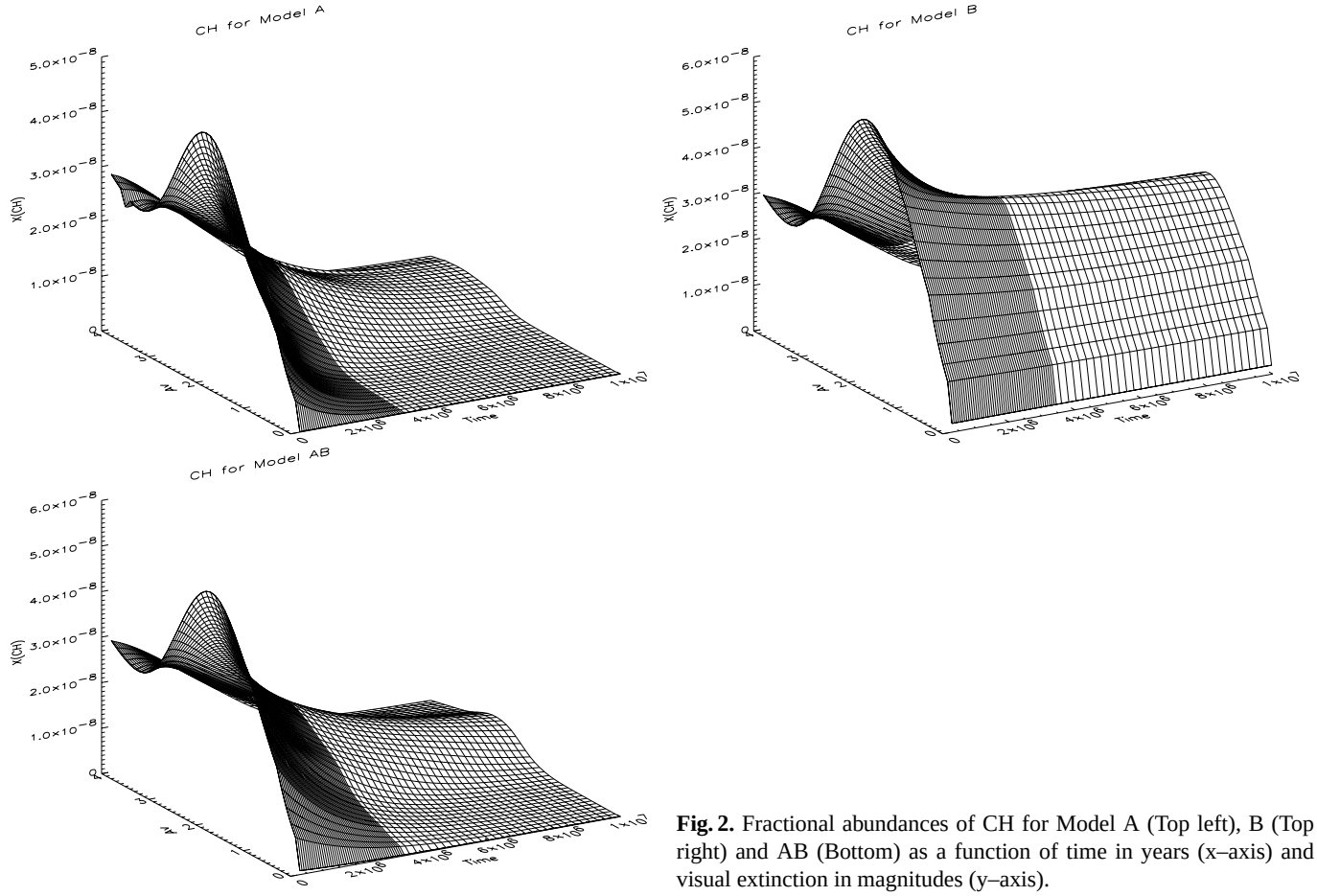

Fig. 2. Fractional abundances of CH for Model A (Top left), B (Top right) and AB (Bottom) as a function of time in years (x–axis) and visual extinction in magnitudes (y–axis).

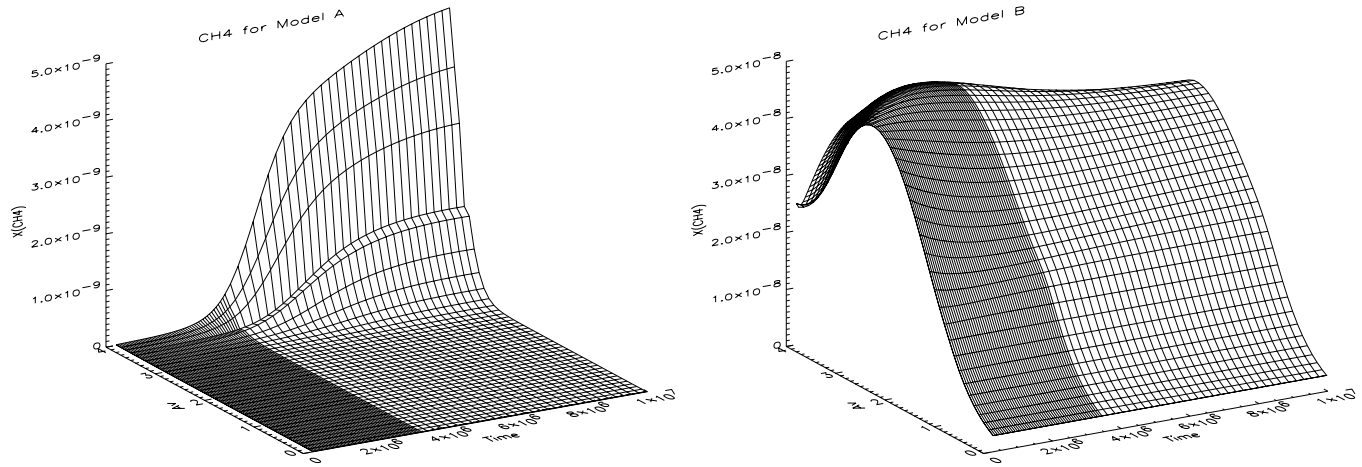

Fig. 3. Fractional abundances of CH_4 for Model A (Left) and B (Right) as a function of time (x–axis) and visual extinction (y–axis).

about 2 orders of magnitude. Also, Turner (1994) observed and modelled H_2CO in clouds with visual extinction of $A_v \sim 1$ to 2 (edge to centre) and found that the gas–phase chemistry failed to reproduce the observed abundances by about four orders of magnitudes. The column densities of H_2CO estimated by our models (see Table 1 and Fig. 4) do not reproduce Turner's observed abundances but they show that there is more than four orders of magnitude difference between Model A and B for A_v = 1 mag. We should note that the clouds observed by Turner (1994) are not necessarily 'diffuse' as their densities and visual extinctions are probably closer to the translucent cloud parameters. We have performed a test run for Model B at n_H = 500 cm^{-3} and found that at A_v = 1.3 mag (cf. Turner 1994) the H_2CO column density is already about three times larger than the value shown in Table 1. These observational results support

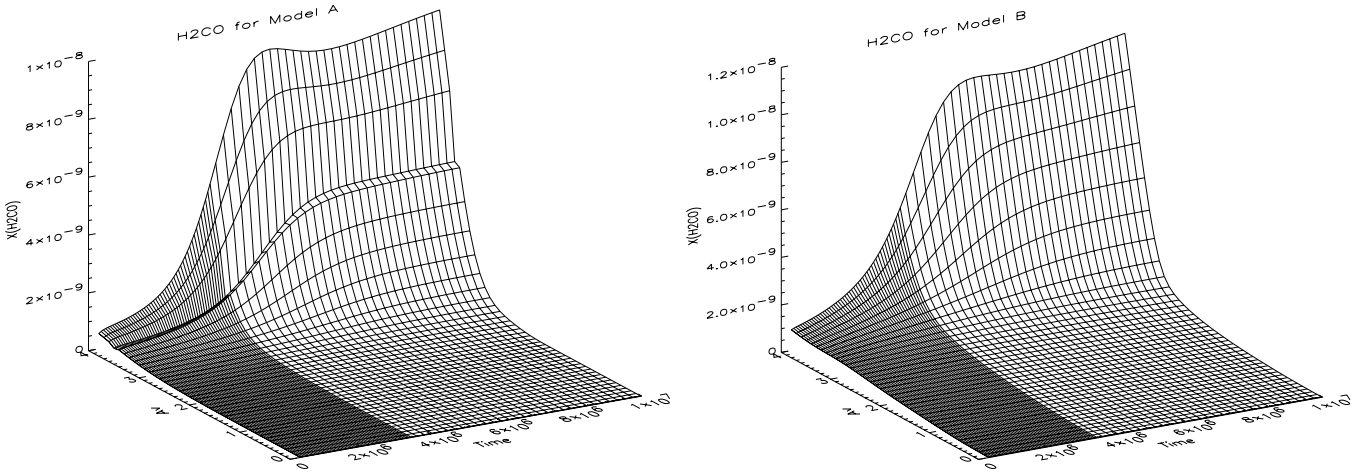

Fig. 4. Fractional abundances of H_2CO for Model A (Left) and B (Right) as a function of time (x–axis) and visual extinction (y–axis).

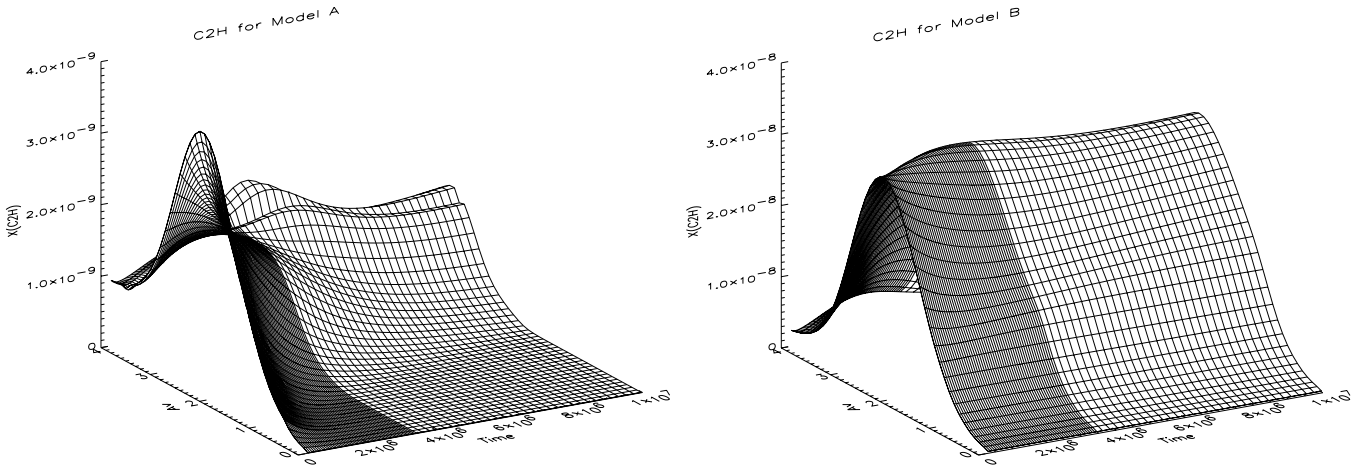

Fig. 5. Fractional abundances of C_2H for Model A (Left) and B (Right) as a function of time (x–axis) and visual extinction (y–axis).

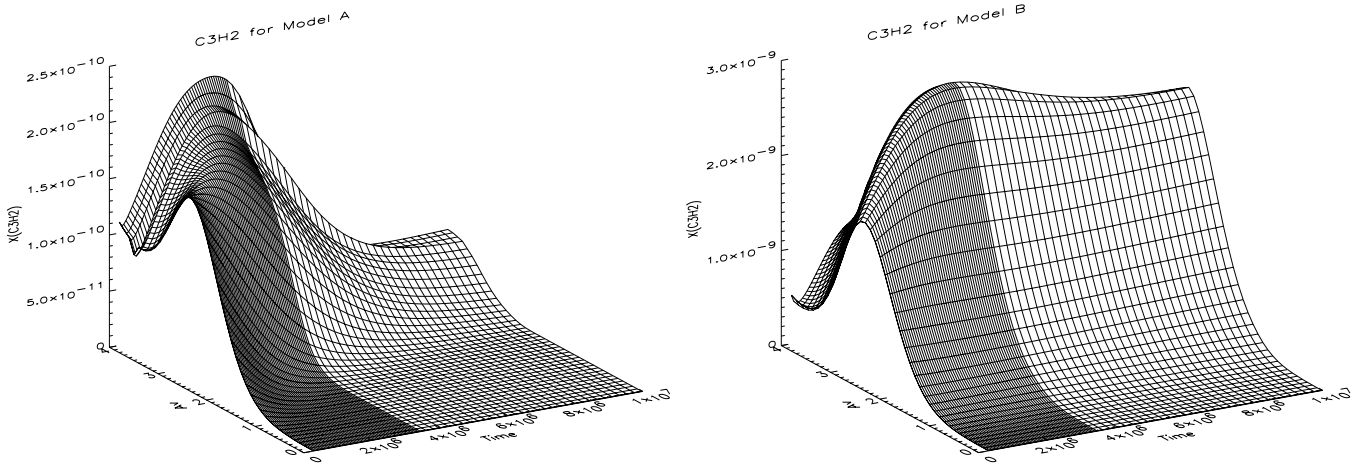

Fig. 6. Fractional abundances of C_3H_2 for Model A (Left) and B (Right) as a function of time (x–axis) and visual extinction (y–axis).

the suggestion that some C^+ might be forming hydrocarbons on grains.

Another photodissociation product of CH_4 is CH_2 which combines with oxygen to form CO. This channel produces more than 30% of the CO in the gas phase in Model B, which will then give a higher abundance of CO than Model A. As CO is one of the most frequently observed molecular species in diffuse clouds, it can be used as another tracer for the formation

Table 1. Derived column densities (cm^{-2}) at 10My of selected species compared, where available, with observed column densities for (1), (3) and (4) which indicate respectively A_v = 1, 3 and 4 mag. A sticking probability (S_x) of 1 for all species and a reduced surface area per unit volume have been adopted. The observed column densities were taken (or derived) as follows: CH (1) from Wagenblast & Williams (1993); CH (3) from Jannuzi et al. 1988; H_2CO (3) derived from Turner (1994); CO (1) from Wagenblast & Williams (1993); CO (3) from van Dishoeck & Black (1991); C_2H (3) derived from Turner, Terzieva & Herbst (1999); C_3H_2 (1) from Cox, Gusten & Henkel 1988; C_3H_2 (3) derived from Turner et al. (1998); CH_3OH (3) derived from Turner (1998).

X	$N(X)_{\rm Model\ A}$	$N(X)_{\rm Model\ B}$	$N(X)_{\rm Model\ AB}$	$N(X)_{\rm Obs}$
CH	6.18×10^{07} (1)	5.62×10^{12} (1)	2.21×10^{10} (1)	$(2.5\pm0.3)\times10^{13}$ (1)
	1.33×10^{12}(3)	5.68×10^{13} (3)	5.65×10^{12} (3)	[a] $(4.6\pm0.8)\times10^{13}$ (3)
	5.03×10^{12}(4)	8.14×10^{13}(4)	1.17×10^{13} (4)	
CH_2	1.12×10^{07} (1)	1.05×10^{12} (1)	5.05×10^{09} (1)	
	1.01×10^{11} (3)	7.65×10^{12} (3)	5.55×10^{11} (3)	
	3.70×10^{11} (4)	1.06×10^{13} (4)	1.05×10^{12} (4)	
CH_3	2.92×10^{06} (1)	4.92×10^{11} (1)	2.24×09^{10} (1)	
	2.32×10^{11} (3)	4.91×10^{12} (3)	7.70×10^{11} (3)	
	1.93×10^{12} (4)	8.68×10^{12} (4)	2.91×10^{12} (4)	
CH_4	— (1)	2.35×10^{12} (1)	4.83×10^{09} (1)	
	5.41×10^{09} (3)	5.92×10^{13} (3)	8.44×10^{13} (3)	
	1.67×10^{12} (4)	1.05×10^{14} (4)	2.30×10^{13} (4)	
H_2CO	7.41×10^{04} (1)	8.27×10^{09} (1)	5.40×10^{07} (1)	
	1.53×10^{11} (3)	5.88×10^{11} (3)	3.12×10^{11} (3)	[b] 5.72×10^{12}
	4.60×10^{12} (4)	5.93×10^{12} (4)	5.25×10^{12} (4)	
CO	3.47×10^{08} (1)	1.59×10^{13} (1)	1.46×10^{11} (1)	$(2.0\pm0.3)\times10^{15}$ (1)
	5.54×10^{15} (3)	3.14×10^{16} (3)	1.01×10^{16} (3)	10^{16}–10^{17} (3)
	4.84×10^{16} (4)	9.26×10^{16} (4)	5.94×10^{16} (4)	
C_2H	— (1)	8.59×10^{11} (1)	1.92×10^{07} (1)	
	9.44×10^{10} (3)	3.75×10^{13} (3)	2.89×10^{12} (3)	1.98×10^{14} (3)
	1.20×10^{12} (4)	5.70×10^{13} (4)	6.66×10^{12} (4)	
C_3H_2	— (1)	5.73×10^{09} (1)	4.31×10^{03} (1)	1.0×10^{12} (1)
	2.74×10^{09} (3)	1.95×10^{12} (3)	1.51×10^{11} (3)	3.0×10^{12} (3)
	4.11×10^{10} (4)	3.06×10^{12} (4)	3.26×10^{11} (4)	
CH_3OH	— (1)	— (1)	— (1)	
	7.87×10^{08} (3)	1.08×10^{08} (3)	3.38×10^{08} (3)	1.8×10^{13} (3)
	1.09×10^{11} (4)	1.03×10^{11} (4)	1.08×10^{11} (4)	

[a] Column density of CH found for one isolated translucent cloud, HD 169454.
[b] Derived column density from fractional abundance for A_v = 1.3 mag.

of hydrocarbons on grains. To date, all models of diffuse clouds had difficulties in reproducing the observed abundance of CO; it has been in general assumed that the main route of CO formation is *via* H_2O and OH. To produce the carbon monoxide, H_2O and OH need to efficiently form on surface grains *via* hydrogenation of oxygen atoms during freeze–out:

$$O_{gas} \rightarrow O_{surface} \rightarrow H_2O \quad \text{and/or} \quad OH \tag{5}$$

The factor limiting the abundance of water and OH in the gas is then the efficiency of reaction 5. Calculations for the ζ Oph cloud model with the revised initial cosmic abundance of oxygen (Savage et al. 1992) showed that the surface reaction 5 should have a high efficiency to reproduce the CO observed (Wagenblast et al. 1993).

For simplicity, we have not included hydrogenation of oxygen in our models, although it seems likely to occur (Williams 1993 and references therein). From Table 1 we note that, although none of the models described in this paper reproduces the observed abundance of CO, Model B comes closest. A combination of Model B and reaction 5 may be able to reproduce the observed CO column density.

In Figs. 5 and 6 we show the abundances of two other species which seem to differ between the models, C_3H_2 and C_2H. C_3H_2 has been detected in low density clouds (Cox, Gusten & Henkel 1988) and their estimate for the column density is shown in Table 1. They find that the typical fractional abundance of C_3H_2 for the diffuse gas is comparable to that measured in dark clouds. For model A, at low visual extinctions, C_3H_2 is only abundant at $\sim$ 10,000 years. The only two efficient ways C_3H_2 can form are:

$$C_2H_2 \xrightarrow{C^+} C_3H^+ \xrightarrow{H_2} C_3H_3^+ \longrightarrow C_3H_2, \tag{6}$$

or

$$C_2H_2 \xrightarrow{C} C_3H \longrightarrow C_3 \longrightarrow C_3^+ \xrightarrow{H} C_3H^+ \xrightarrow{H_2} C_3H_3^+ \longrightarrow C_3H_2, \tag{7}$$

and C_2H_2 is an indirect product of CH_4 through reactions such as

$$CH_4 \xrightarrow{C^+} C_2H_3^+ \xrightarrow{e} C_2H_2. \quad (8)$$

Model B predicts a lower abundance than observed; however, it is constant with time, and the observed abundance derived by Cox, Gusten & Henkel is for densities that could be higher than 300 cm^{-3}. In fact, at n_H = 500 cm^{-3} Model B predicts an increase in the column density of C_3H_2 by about a factor of three.

C_2H (Fig. 5) is a photodissociation product of C_2H_2 whose abundance depends on C^+ and CH_4. Model A shows that pure gas–phase networks will not produce detectable amounts of C_2H for low visual extinction clouds, while Model B produces detectable abundances even at low extinction. Detections of C_2H have not yet been published but recent observations (Liszt & Lucas 1999) reveal that it might be present in diffuse clouds in fractional abundances comparable to those detected in dark clouds.

A large part of the difference between the models can be attributed to the significant reduction in the total amount of carbon frozen out over the lifetime of the cloud: In Table 2 we present computed results of N(CH) cm^{-2} and N(C^+) cm^{-2} for single point (A_v = 1) models in which the grain interaction terms are modified. The product of the sticking probability, S_x, and the grain surface area per unit volume, G, (where G = 1 corresponds to the canonical grain size distribution) is shown in the table for several cloud ages, for a cloud with A_v = 1. These results confirm that Model A is incapable of providing the observed abundances of CH (and C^+), regardless of the cloud age or gas/grain interaction. Note that the column densities estimated in Table 2 are approximate values as they are calculated by simply multiplying single point fractional abundances by the column density of molecular hydrogen at A_v = 1 mag.

Table 2. Observed column densities (from Wagenblast & Williams 1993) for CH and C^+ at A_v = 1 mag compared with estimated column densities from Models A, B and AB for different values of S_xG [It is normally assumed that $0 \lesssim S_x \leq 1$; G = 1 corresponds to the canonical grain size distribution].

		CH	C^+
	Obs	$(2.5\pm0.3)\times10^{13}$	$(9.3\pm4.5)\times10^{16}$
		S_xG = 0.3	
A	3My	9.02×10^{12}	2.53×10^{16}
A	5My	3.20×10^{12}	9.05×10^{15}
A	10My	2.98×10^{11}	8.68×10^{15}
B	3My	3.40×10^{13}	9.72×10^{16}
B	5My	3.20×10^{13}	9.72×10^{16}
B	10My	2.99×10^{13}	9.66×10^{16}
AB	3My	1.82×10^{13}	5.04×10^{16}
AB	5My	1.09×10^{13}	3.07×10^{16}
AB	10My	3.50×10^{12}	9.70×10^{15}
		S_xG = 0.5	
A	3My	3.59×10^{12}	9.72×10^{15}
A	5My	6.14×10^{11}	1.71×10^{15}
A	10My	1.17×10^{10}	3.40×10^{13}
B	3My	3.62×10^{13}	9.67×10^{16}
B	5My	3.39×10^{13}	9.64×10^{16}
B	10My	3.15×10^{13}	9.51×10^{16}
AB	3My	1.24×10^{13}	3.18×10^{16}
AB	5My	5.28×10^{12}	1.36×10^{16}
AB	10My	7.41×10^{11}	1.93×10^{15}
		S_xG = 0.7	
A	3My	1.38×10^{12}	3.69×10^{15}
A	5My	1.15×10^{11}	3.22×10^{15}
A	10My	4.63×10^{8}	1.32×10^{12}
B	3My	3.83×10^{13}	9.61×10^{16}
B	5My	3.58×10^{13}	9.55×10^{16}
B	10My	3.31×10^{13}	9.37×10^{16}
AB	3My	8.27×10^{12}	1.98×10^{16}
AB	5My	2.44×10^{12}	5.95×10^{15}
AB	10My	1.54×10^{11}	3.84×10^{15}
		S_xG = 1	
A	3My	3.21×10^{11}	8.57×10^{15}
A	5My	9.51×10^{9}	2.62×10^{13}
A	10My	3.59×10^{6}	1.01×10^{10}
B	3My	4.14×10^{13}	9.51×10^{16}
B	5My	3.85×10^{13}	9.42×10^{16}
B	10My	3.54×10^{13}	9.14×10^{16}
AB	3My	4.37×10^{12}	9.72×10^{15}
AB	5My	7.53×10^{11}	1.71×10^{15}
AB	10My	1.47×10^{10}	3.41×10^{13}

3.2. Translucent clouds

The column densities of several molecular species in translucent clouds are large enough for millimeter–wave observations to be feasible. CH in particular has been extensively surveyed (Magnani et al 1989; van Dishoeck & Black 1989) and modelled (van Dishoeck & Black 1989). In Table 1 we report the observed and estimated column density for A_v = 3 and 4 mag. Model B, at A_v = 3 mags, is much closer to the observed value than the other two models. However, CH column densities measured for translucent clouds vary along different lines of sight by more than one order of magnitude. The observed value cited in Table 1 is closer to the lower limit and therefore more representative of our models where the density is quite low. Model A is always, except at early times, underabundant in CH. Note, however, that CH is still high at late times with respect to the diffuse cloud case. In fact, at high visual extinctions, CH_4 is abundant for Model A (see Fig. 3), in spite of reaction (1) being switched off, because as visual extinction increases the cloud is more shielded from photodissociation and carbon is retained in its neutral form in the gas and easily forms CO. Both carbon and carbon monoxide react with CH_5^+ and form CH_4, in alternative routes to reaction 1.

As in the case of diffuse clouds, we find a time–dependence for the chemistry of translucent clouds. C^+ is still crucial for the formation of CH: as we increase the visual extinction C^+, the dominant form of carbon at the edge of the cloud, is transformed

into C and CO, but we find that C^+ is not totally negligible until $A_v \geq 4$ mag.

To test the hypothesis that the chemistry of translucent clouds is time–dependent and that depletion of carbon may be important, more complex hydrocarbons and H_2CO can be used as observational tracers. H_2CO has been detected in several translucent clouds (e.g. Magnani et al. 1996; Turner 1994); its column density is shown in Table 1. None of the models reproduces the observed abundances precisely, although again Model B is the closest. However, the density we have adopted is probably a lower limit for translucent clouds, and higher densities will increase the H_2CO fraction (see above).

C_3H_2 has been detected in many sources (Turner et al. 1998) with visual extinctions A_v = 2.4 $\sim$ 5.2 mag. The 'new standard model', for $A_v \geq 3.6$, of Lee et al. (1996) underestimates the observed column density of C_3H_2 by at least a factor of 10. The C_3H_2 column density in Model B, at A_v = 3 mags, is very close to the observed column density while Model A is underabundant by three orders of magnitude.

C_2H has been observed, together with other species, by Turner et al. (1999). They found surprisingly strong lines, and inferred an average fractional abundance of 6.6×10^{-8} which for $A_v \sim 3$ mag corresponds to a high column density (see Table 1). Our models do not reproduce such a high column density but our computed abundance for Model B at A_v = 4 mag is within a factor of four of the observed value. Static models only manage to fit the observed value with densities higher than 1000 cm^{-3} and carbon to oxygen ratio close to unity (Turner et al. 1999).

Other hydrocarbons recently observed in translucent clouds include CH_3OH (Turner 1998). He finds that its column density cannot be reproduced with 'new standard models' which underestimate it by at least 4 orders of magnitude. Our models also underestimate its abundance. Turner suggests that methanol might form by energetic processing (UV and cosmic rays) of CO ice on grains followed by UV photodesorption of methanol. Formation of methanol on grains has been considered for denser environments (e.g. Caselli et al. 1993).

4. Conclusions

We have investigated the viability of models of diffuse clouds in which the interaction of C^+ ions with dust grains is presumed to play a significant part. The ions are supposed either to be incorporated in hydrogenated amorphous carbon mantles (as required by one class of grain models) or to be hydrogenated at the surface and provide a source of CH_4 in the gas phase (by analogy with nitrogen, following recent studies of interstellar NH). We have computed the time–dependent abundances of various hydrocarbons and other species, and compared these with column densities inferred from observations of both diffuse and translucent clouds.

Assuming that diffuse clouds are about 10My old, then it seems clear that incorporation of much of the C^+ in HAC on this timescale is not viable, as insufficient amounts of CH are produced. On the other hand, if much of the C^+ arriving at grain surfaces is hydrogenated, then significant amounts of CH_4, and derivatives therefrom, should be produced. In particular, detectable column densities of H_2CO, C_3H_2, and C_2H should arise, even in diffuse clouds (assuming these are represented by $A_v \lesssim 1$). Therefore, the assumption of hydrogenation of C^+ is clearly testable by observation of these products.

There is a significant shortfall in the computed CO column density for diffuse clouds. This may be addressed by adjustment of the (unknown) C^+ recombination rate at low temperatures (Wagenblast & Williams 1993). On the other hand, if oxygen as well as carbon is hydrogenated at grain surfaces, then the discrepancy may disappear. A computation is in progress of chemistry in which surface hydrogenation is extended to all atomic species, to test this and other points.

Our models have been extended to visual extinctions appropriate for translucent clouds, though the gas number density has been retained at a rather low value for such objects. The results of these models have been compared with column densities inferred from observations. In general, there is reasonable agreement between computed and observed column densities for several hydrocarbons, in the case that hydrogenation of the carbon to CH_4 is occurring. Models in which much of the carbon is incorporated as HAC fail to account for the observed hydrocarbon abundances. It seems unlikely that the discrepancies could be removed by a modest change in number density or in visual extinction.

Methanol has been detected in translucent clouds, but none of the models investigated here is viable, unless high density and high A_v are both invoked. However, it seems likely that a direct surface mechanism, such as hydrogenation of CO, may need to be invoked, if the number density and A_v adopted are reasonably appropriate. Such a process for CO is, of course, routinely invoked in models of hot cores.

We conclude that models in which significant fractions of available carbon are trapped in HAC mantles on a timescale of 10My are not viable, from a chemical viewpoint. On the other hand, hydrogenation of much of the carbon incident on grain surfaces can provide an explanation of the origin of some polyatomic molecules in diffuse and translucent clouds. The detection of C_2H and C_3H_2 along diffuse lines of sight with well-defined physical conditions should define the efficiency of processes described here.

There are alternative ways of accounting for abundances of hydrocarbons in diffuse and translucent clouds. For example, models involving turbulence–driven reactions (e.g. Spaans 1995; Turner, in preparation) also show high efficiency in producing CH, CH^+ and other species in the gas phase. There may, however, be some differences in the chemistry to be expected from the turbulence model and that from the surface chemistry model explored here.

Acknowledgements. SV would like to acknowledge the financial support of a PPARC post–doctoral research assistantship. DAW is grateful to PPARC for the award of a Senior Fellowship. PTO acknowledges the financial support of a PPARC studentship. The authors thank the referee for very helpful comments.

References

Caselli P., Hasegawa T.I., Herbst E., 1993, ApJ 408, 548
Cecchi–Pestellini C., Williams D.A., 1998, MNRAS 296, 414
Cox P., Gusten R., Henkel C, 1988, A&A 206, 108
Crawford I.A., Williams D.A., 1997, MNRAS 291, 53L
Danks A.C., Federman S.R., Lambert D.L., 1984, A&A 130, 62
Drdla K., Knapp G.R., van Dishoeck E.F., 1989, ApJ 345, 815
Jannuzi B.T., Black J.H., Lada C.J., van Dishoeck E.F., 1988, ApJ 332
Jones A.P., Duley W.W., Williams D.A., 1990, QJRAS 31, 567
Lambert D.L., Danks A.C., 1986, ApJ 303, 401L
Lee H.-H, Bettens R.P.A., Herbst E., 1996, A&AS 119, 111
Liszt H.S., Lucas R., 1999, A&AS 194, 4103
Magnani L., Lada E.A., Sandell G., Blitz L., 1989, ApJ 339, 244
Magnani L., Onello J.D., 1993, ApJ 408, 559
Magnani L., Caillault J.-P., Hearty T., et al., 1996, ApJS 106, 447
Millar T.J., Farquhar P.R.A., Willacy K., 1997, A&AS 121, 139
Rawlings J.M.C., Hartquist T.W., Menten K.M., Williams D.A., 1992, MNRAS 255, 471
Savage B.D., Cardelli J.A., Sofia U.J., 1992, ApJ 401, 706
Semaniak J., Larson A., Le Padellec A., et al., 1998, ApJ 498, 886
Snow T.P., Witt A.N., 1996, ApJ 468, 65L
Snow T.P., Black J.H., van Dishoeck E.F., et al., 1996, ApJ 465, 245
Spaans M. 1995, Ph.D. Thesis
Turner B.E., Lee H.-H., Herbst E., 1998, ApJS 115, 91
Turner B.E., 1994, ApJ 437, 658
Turner B.E., 1998, ApJ 501, 731
Turner B.E., Terzieva R., Herbst E., 1999, ApJ 518, 699
van Dishoeck E.F., Black J.H., 1989, ApJ 340, 273
van Dishoeck E.F., Black J.H., 1991, ApJ 366, 141
van Dishoeck E.F., 1998, In: Hartquist T.W., Williams D.A. (eds.) The molecular astrophysics of stars and galaxies. Oxford Science Publications, Oxford, p. 53
Wagenblast R., 1992, MNRAS 259, 155
Wagenblast R., Hartquist T.W., 1988, MNRAS 230, 363
Wagenblast R., Williams D.A., Millar T.J., Nejad L., 1993, MNRAS 260, 420
Wagenblast R., Williams D.A., 1993, In: Millar T.J., Williams D.A. (eds.) Dust and Chemistry in Astronomy. IOP Publishing, Bristol, p. 171
Wagenblast R., Williams D.A., 1996. Ap&SS 236, 257
Williams D.A., 1992, Planetary and Space Science 40, 1683
Williams D.A., 1993, In: Millar T.J., Williams D.A. (eds.) Dust and Chemistry in Astronomy. IOP Publishing, Bristol, p. 143